Direct Measurements of Minimum Detectable Vapor Concentrations Using Passive Infrared Optical Imaging Systems

Paper # 1025

Robert G. Benson[†a], Jeffrey A. Panek[‡b], Paul Drayton[b]
[a]Flir Systems Inc, 25 Esquire Rd., North Billerica, MA. USA 01862
[b]Innovative Environmental Solutions, P.O. Box 177, Cary IL. USA 60013-0177

ABSTRACT

Passive infrared imagers designed to detect and visualize physical materials such as vapors and mists via their infrared spectral absorption have been tested and characterized using self contained gas cells. Techniques and test methods are discussed and results are shown for a subset of imagers and vapors tested. Theoretical foundations and the statistical treatment of the data and the associated results are presented.

Keywords: Infrared, spectral absorption, optical imaging, vapor imaging, gas cells, absorbance, GasFindIR.

1. INTRODUCTION

Passive standoff infrared optical imaging systems such as FLIR's GasFindIR™ have become essential tools in the field of spectral imaging[1]. Vapors or mists whose spectral characteristics prohibit detection in visible wavelengths may be detected in the infrared by utilizing their inherent scattering and absorbing properties. Direct applications of this technology include leak detection and repair,(LDAR), atmospheric hydrodynamics, and materials research. It is therefore imperative to accurately measure the concentrations of material that these passive systems can optically detect. At present there is no widely accepted methodology or set of standards and practices to determine these quantities in a laboratory setting. We present a test method and procedure that could be utilized for nearly every type of passive optical imaging system. The resultant data may be used to accurately measure and quantify an imaging system's ultimate sensitivity to a spectrally absorbing vapor or mist.

1.1 Spectral Absorbance

The commonly accepted definition of absorbance is the base 10 logarithm of the ratio of initial intensity to final intensity of light passing thru an absorbing material. One can also use the relationship of an absorption coefficient over a concentration path length to denote or mathematically represent the quantity of absorbance.

$$I_o = I * 10^A \quad \text{and} \quad A = k * C * l \tag{1}$$

[†] Email bob.benson@flir.com
[‡] Email japanek@ameritech.net

Where A is the absorbance measured at concentration C over optical path length l. k is the associated absorption coefficient.

We have not explicitly denoted the wavelength dependence of A. Under certain circumstances one may approximate the absorbance of a substance at different concentrations and over other path lengths then were directly measured. This approximation may be linear to first order and only holds true under certain physical conditions. In our test methods section we show where and under what conditions this linear approximation eventually breaks down. To compute the absorbance of a vapor whose desired concentration is 10 times that at which the spectral absorbance has been measured one would simply multiply the measured absorbance, A, by 10. See Figure (1) for an example absorbance of methane. In the figure, the path length is 2.25m and the concentration is 400 ppm, (parts per million).

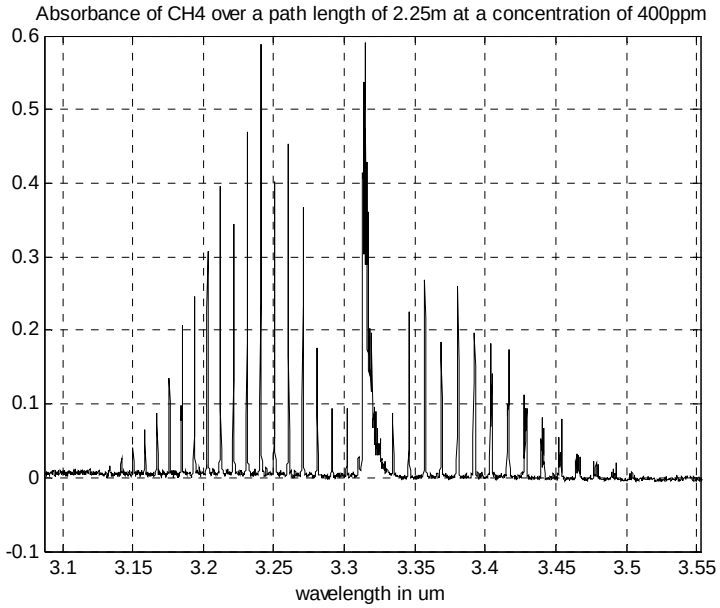

Figure 1. Spectral absorbance data taken from the online spectral database hosted by the EPA[2].

1.2 Monochromatic Radiance

The radiant emittance considered here, and used in the test method, is blackbody radiation. Forward looking thermal imagers are inherently polychromatic, ie. bandpass imagers. It is useful to consider the monochromatic nature of the physical process first and then extend the results to a spectral bandpass. Consider the Planck radiation function and the photonic flux incident on a detecting pixel in the thermal imager. The irradiance of light at any given wavelength falling on the pixel is then given by,

$$R_\lambda(T) = \frac{B_\lambda(T)}{\pi} \cdot \Omega \cdot \mathrm{A} \tag{2}$$

Where A is the area of the pixel, Ω is the solid angle subtended by the pixel and $B_\lambda(T)$ is the planck function. In a photon counting infrared focal pane array, (FPA), we may estimate the total signal in electrons generated by this irradiance for the center pixel[3].

$$S_\lambda(T) = \frac{\lambda}{hc} B_\lambda(T) \cdot \mathrm{A} \cdot itime \cdot QE_\lambda \Big/ 4 \cdot F_\#^2 \quad (3)$$

Where QE is the FPA's external quantum efficiency, itime is the integration time of the sensor, and $F_\#$ is the optical speed of the imager[§].

In a background limited camera system the shot noise associated with this signal may be approximated by poisson statistics[4].

1.3 Detection of the Vapor

In many optical imaging applications the minimum detectable signal is defined by the ratio of signal to noise in the camera. When the signal to noise ratio is unity it is considered the minimum signal that can be detected by the camera. In this test method, the vapor acts as an attenuator of photonic signal from the illuminating source blackbody. As such one can mathematically compute when the signal loss due to photons being absorbed by the vapor is equal to the shot noise associated with the photonic signal itself from the blackbody, such that a signal to noise ratio of unity will be achieved. This would then constitute the minimum detectable absorbance of that vapor by the camera. Mathematically, it may be described using eqs(1) and (3),

$$\frac{Signal}{Noise} = \frac{S_\lambda(T) \cdot (1 - 10^{-A_\lambda})}{\sqrt{S_\lambda(T)}} = \sqrt{S_\lambda(T)} \cdot (1 - 10^{-A_\lambda}) = 1 \quad (4)$$

Here we have explicitly shown the wavelength, λ, dependence of the absorbance, and have assumed a background limited system.

1.4 Estimation of the Absorbance

The dependence of absorbance on concentration may be extracted from eq(1) and we may envision an experiment to directly measure the imager's sensitivity to the vapor's absorbance using eq(4) as the condition upon which the minimum detectable threshold is met. Rather then calculating the noise in the camera from eq(3) we may use digitizing video processing equipment to perform direct measurements of both the camera's noise and signal levels. These may then be compared to our theoretical estimations derived above.

2. EXPERIMENTAL METHODS AND TECHNIQUES.

2.1 Measurement of the Absorbance

To accurately measure the minimum concentration of a vapor detectable with the GasFindIR an experimental technique using gas cells was devised. Since the amount of IR optical attenuation that a vapor will introduce is dependent on both concentration and path length from eq(1), the path length of the cells used was fixed at 1 meter. Additionally, since the signal change generated by this attenuation is proportional to the temperature of the illuminating source, i.e. the blackbody, a constant temperature source was deployed. The bandpass of the GasFindIR is not optically variable, there is therefore no wavelength variation inherent the experiment. With these quantities fixed

[§] For all other pixels in the FPA, the solid angle is simply multiplied by a cosine function, we shall forsake that treatment for the sake of simplicity.

throughout the testing one can define a precise mathematical relationship between the concentration of the vapor and the amount of attenuation that concentration will generate in the camera. Hence,

$$\Delta S = \int_{Bandpass} S_{\lambda}(T)(1-10^{-A_{\lambda}})d\lambda \quad (5)$$

If we assume a simple linear relationship between absorbance and concentration then one may predict signal attenuation. This is, as mentioned earlier, a perilous assumption for large variations of concentrations.

A measurement of the signal attenuation for various concentrations of a single vapor should lead to a predictable relationship confirmed by direct measurements. Since signal attenuation can be fit functionally using measurable data taken at known concentrations one can easily determine when this signal will be equal to the measured noise floor in the camera satisfying the criteria for detection stipulated in eq(4).

2.2 Experimental Setup

The experiment was conducted and hosted by British Petroleum at their Naperville, Illinois research and development facility. The laboratory space was provided at no cost by BP[**] and is maintained in cooperation with IES.

A simple one meter path length stainless steel gas cell was used to house the vapor at constant concentrations. The cell was outfitted with Anti-Reflective,(AR) coated Zinc Selenide bandpass windows at both ends, as shown in figure 2. The windows were mounted with O-rings to ensure an air tight seal. The imaging system looked through the front window of the cell tube and out through the rear of the cell where a blackbody was placed that filled the rear window's aperture, as shown in Figure (2). The vapor flowed through the cell via steel fill and purge tubing. The flow volume and concentration was controlled via an environics mass flow controller[5].

The camera system was positioned such that the exit aperture on the gas cell subtended a significantly large amount of the camera's overall field of view, covering many thousands of pixels on the FPA. The video output of the camera was digitally captured using a COTS 10-bit frame grabber and simulteanously sent to a digital oscilloscope so the experimenters could easily maintain usable video levels. The frame grabber's data was stored on a PC and imaging data manipulation software from Santa Barbara Infrared was used to generate signal averages and noise levels.

[**] The authors would like to recognize and commend British Petroleum and our host David Fashimpaur for the use and access to the R+D facilities in Naperville, IL.

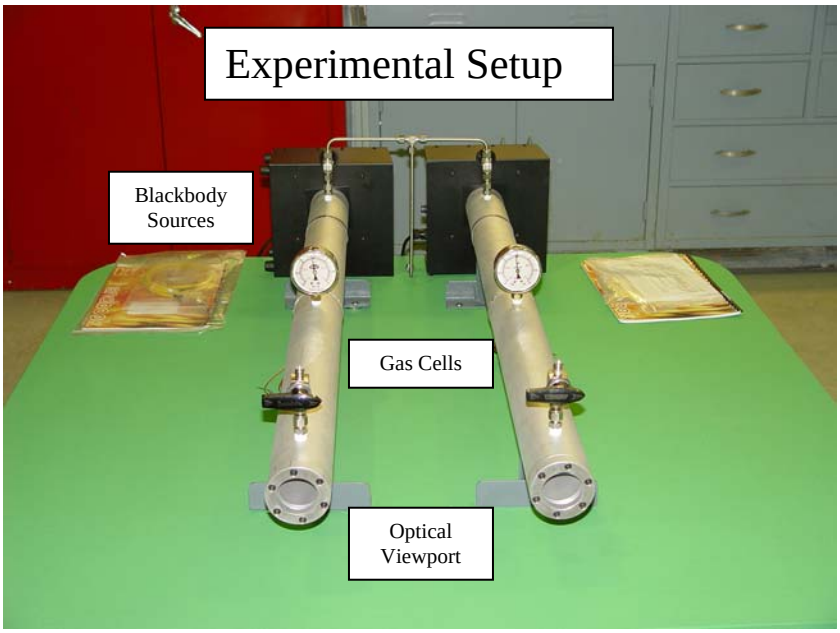

Figure 2. Typical experimental setup. Sealed gas cells with controlled blackbody sources.

The environment in the lab space was not tightly controlled. Air temperatures rose and fell during these tests. To ensure accuracy in the data collected, measurements were made both before the cells were filled and after they were purged to correct for any signal that was induced from temperature drift in the materials along the optical path.

3. MEASUREMENTS AND DATA REDUCTION

3.1 Data Collection and Measurements

Prior to collecting attenuation data, the camera's noise floor was established in A/D counts, (ADUs) at the frame grabber. The camera was placed in manual mode so that it's maximum video output gain level was set and fixed throughout the test. A series of 32 consecutive frames of data was taken. The standard deviation of each pixel's signal over time was calculated. The mean value of the standard deviations for many pixels was computed. This is the camera's temporal noise floor. Since the camera's spatial noise is much less then the temporal noise we have omitted any impact of spatial noise in this test.

The output video level of the camera was adjusted such that the blackbody being viewed was well within the dynamic range of the frame grabber. Data points of the camera's output signal were collected every 20 seconds for approximately 2 minutes to establish an initial background level. The gas was then introduced to the cell. Data continually logged every 20 seconds during this process. Once the gas had mixed and displaced the original air in the cell several data points were taken, again every 20 seconds. The cell was then purged with nitrogen and data were collected to produce a final background level, as shown in figure 3.

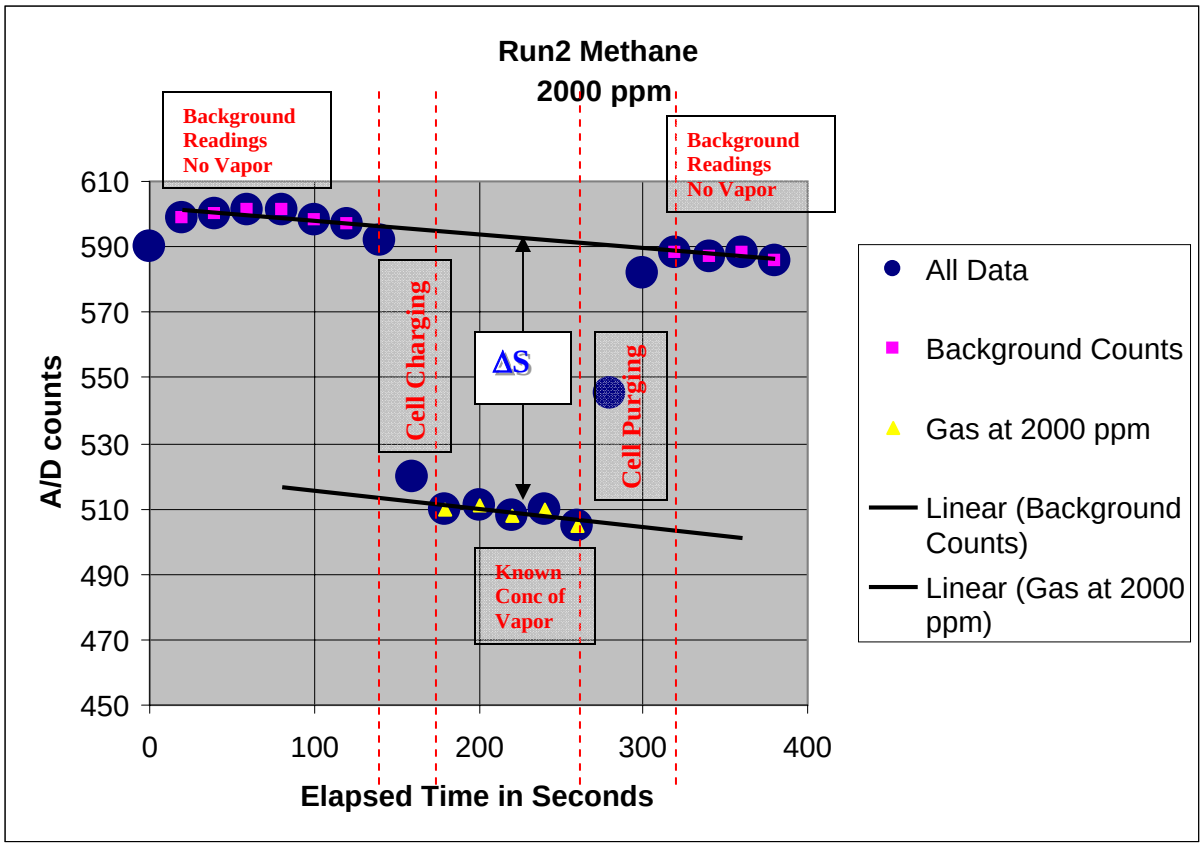

Figure 3. Measurement of the signal attenuation from 2000ppm of Methane.

This process was repeated for different concentrations of a single species of gas. In each case the signal attenuation was calculated for each concentration tested.

3.2 Data Reduction

Each concentration produced a data set similar to that shown in Figure 3. The data were fit to determine background and final attenuated signal levels. The background levels were subtracted from the attenuated signal levels to produce an overall change in signal response due to the absorbing gas. Error estimates were derived at the 99th % confidence level of the T-distribution. The error in concentration present was estimated from the environics controller literature.

Data were reduced for a variety of concentrations and results are shown in figure 4.

3.3 Data Repeatability

To verify the experimental repeatability of this method, the same concentration of the same gas was collected at different times and reduced. Figure 5 shows two data sets of methane at 1000ppm each taken on differing days. The reduced signal attenuations agree to within the experimental errors giving the authors confidence in the data collected and presented .

4. ANALYSIS AND DISCUSSION

4.1 Data Analysis

Using the measured values of the S/N ratio over several concentrations a simple transcendental functional was fit to the data. The derivation of this function is an entirely empirical fit to the data. While a theoretical derivation of the functional form may be possible, it may not result in a closed form equation, and it will certainly differ from species to species. The derivation of this from fundamental principles doesn't result in any new knowledge and therefore has been avoided by the authors. The functional we found best fit the data is shown in eq(6) and plotted in figure(6).

$$\frac{S}{N}(C) = \alpha \cdot \log 10(C) + \beta \cdot C + \chi \qquad \text{eq(6)}$$

Where α, β, and χ are fitted parameters. The fit results in a R^2 of 0.9997 indicating an excellent agreement with the data[6]. Using the function given in equation 6, we extract the methane concentration necessary to achieve a signal to noise ratio of unity in the camera. This value was 275 ppm*m after correcting for the cell window's optical transmission.

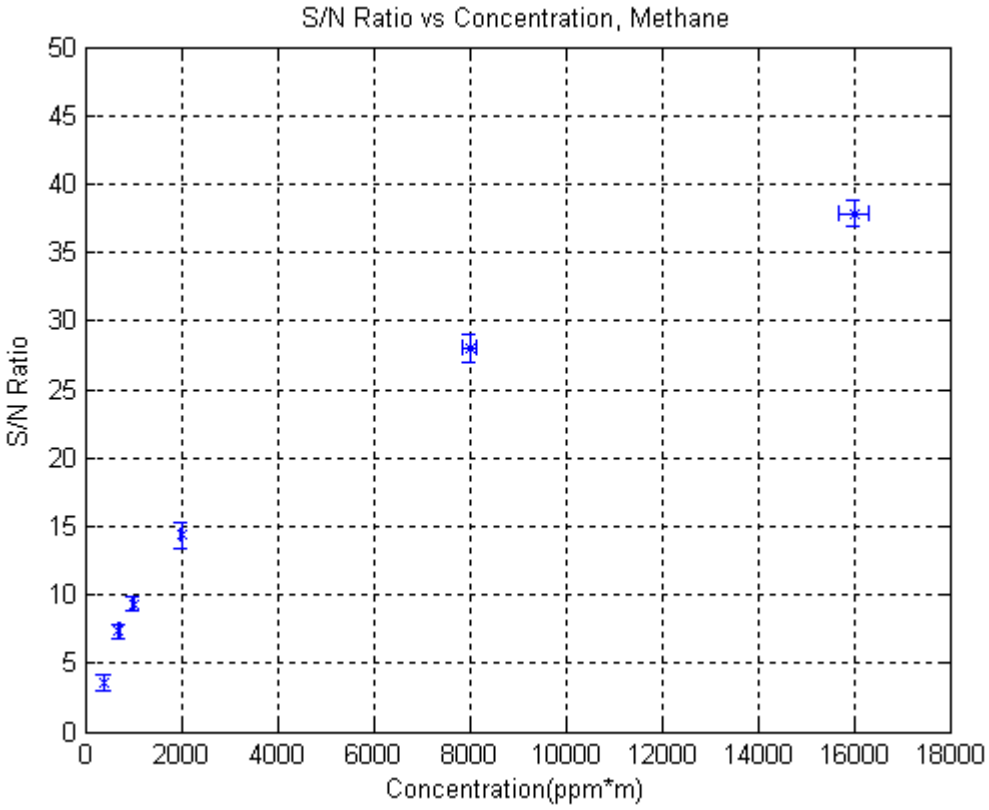

Figure 4. Signal Attenuation vs. Gas Concentration.

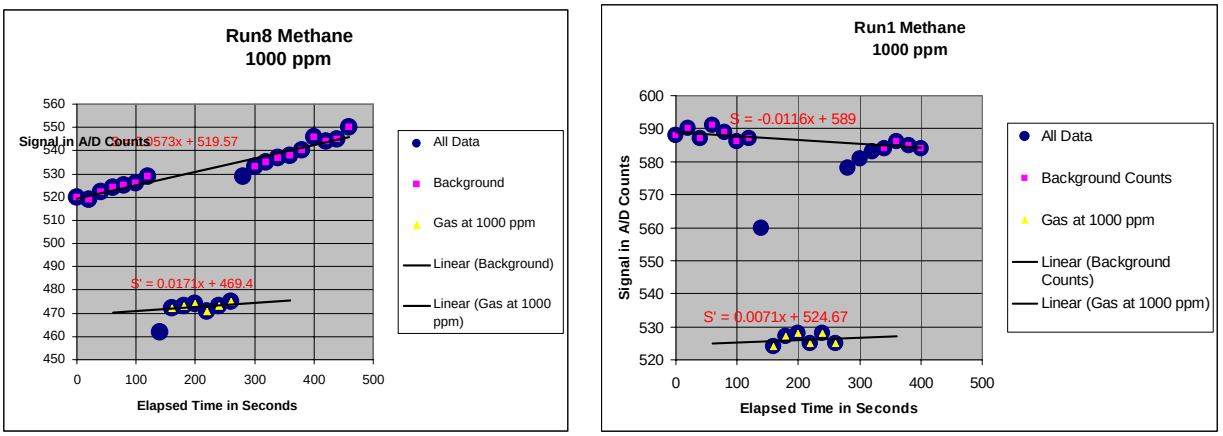

Figure 5. Test method repeatability. Run8 is 58.6+-3.38 ADU, Run 1 is 60.4+-4.24 ADU. These are well within the experimental error bars of one another and demonstrate a day over day repeatability of the test method.

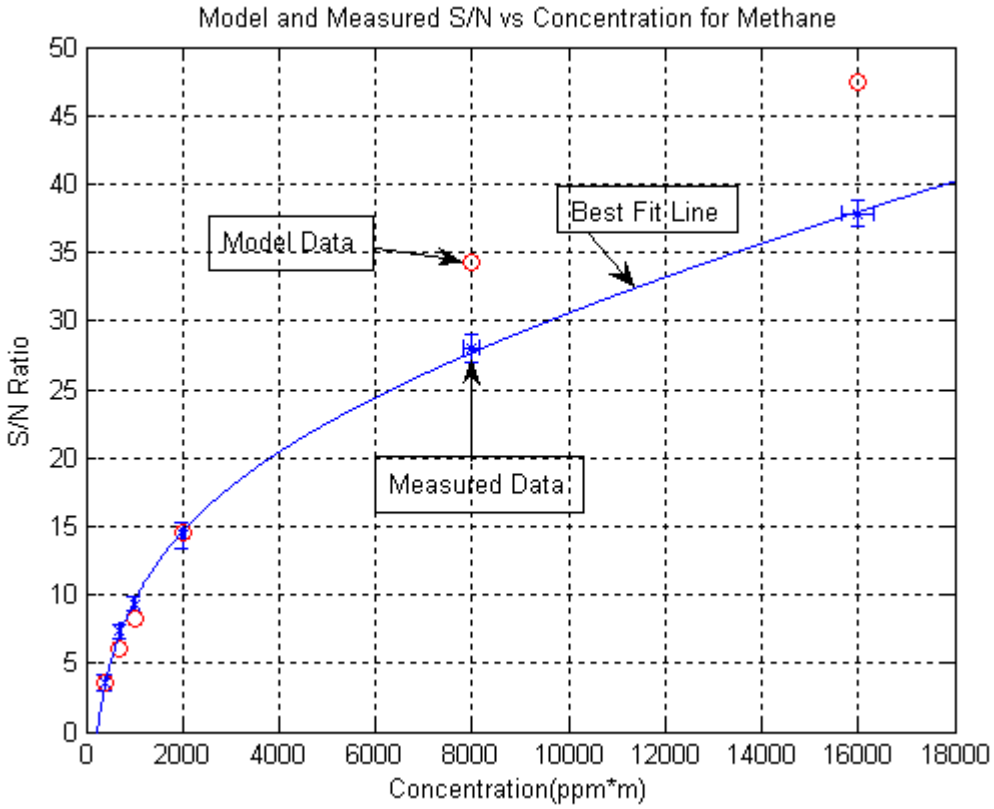

Figure 6. Modeled and Measured S/N,

4.2 Data Modeling

A sensitivity model of the tested camera was developed in an effort to independently verify and predict the S/N ratios that were measured. The model predictions are plotted in figure(6). The

model uses as an input the expected spectral transmission of the vapor over the 1 meter path length at a given concentration. It is therefore highly dependent upon the input spectrum. For the model, the chosen input spectrum was a calculated one, as opposed to an actual measured spectrum, which was drawn from the EPA's spectral database. The calculated spectrum was used for several reasons, including low background,(measurement) noise, spectral resolution, and concentration path length. The calculated spectrum was generated for a vapor concentration of 1.68ppm over a path length of 30 meters at a temperature of 300K. This leads to a concentration path length of 50.4ppm*m and is quite close to the lowest concentrations we used in our experiment. At higher concentrations the linear approximation scheme begins to incur significant errors.

As the concentration of the vapor changed new absorbances were calculated based upon the 1 input spectrum. Spectral transmissions were generated from those linearly approximated absorbances. See figure(8). Note as the concentrations rise the obvious noise generated in the transmission also rises, this gives way to a false overestimate of the spectral absorbance.

The spectrum downloaded and used from the EPA's database seemed to have higher absorbances when compared to other actual measured spectra. We have no explanation for this however since we were mathematically manipulating the spectrum perhaps the linear approximation used lead to this discrepancy. As we input this spectrum into our model we found we had to reduce the overall absorbance by a factor of 4.4 in order to achieve a fit to the experimental findings. We believe this is likely due to a combination of factors, including computational evaluation of the integrated transmission, assumptions of the spectral absorbance on concentration, and camera performance metrics.

4.3 Discussion of the Data

We see from the transmission plots in figure (8) where obvious errors in the model may originate. The plots themselves are still quite useful as tools to interpret the S/N data shown in figure(7). As the concentrations begin to rise we see the S/N following a logarithmic and then more linear relationship. This is due to the individual spectral lines falling into saturation with respect to their monochromatic transmission. If an individual spectral line has essentially brought to extinction a particular wavelength of source photons, then it simply won't boost S/N to have higher concentrations of the gas. The line is already attenuating all the photonic energy at that particular wavelength, simply adding vapor has no effect. The imager as stated earlier is a bandpass imager and thus integrates spectrally across the viewable bandpass. The exact specifications of the bandpass are proprietary, however one can see how ever increasing concentrations lead to ever decreasing slopes of the S/N. Once individual lines have been brought to extinction their contribution to the integrated attenuation significantly diminishes. The lines only continue to contribute in the line wings which don't change nearly as much with concentration as the line centers.

The experimental results show a highly predictable data set. The errors incurred are relatively small and don't have tremendous influence over the end results. The errors could be significantly reduced in the future however there is always a cost benefit trade which must be made.

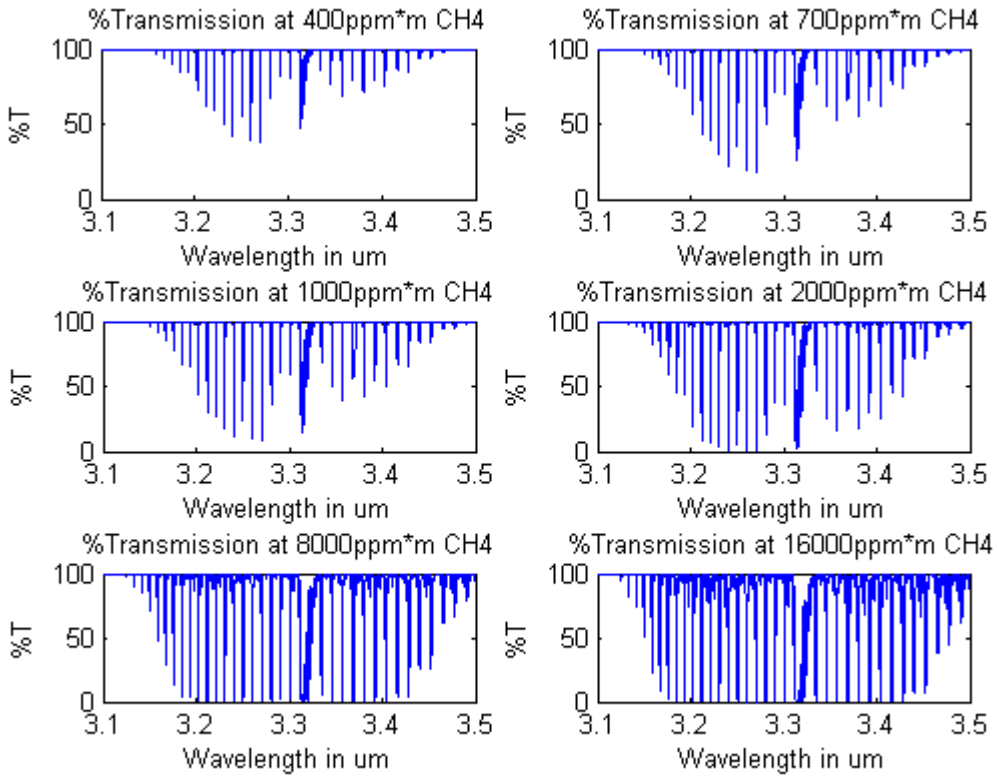

Figure 8. Spectral transmission approximations at various vapor concentrations.

5. CONCLUSIONS

In this paper we have demonstrated a new method and experimental process that could be used across the board to measure the vapor sensitivity of thermal imagers. This work could be extended to leak rates developing minimum detectable leak rates based on measured minimum detectable concentration path lengths. This work also shows conclusively how a vapor's concentration path length relates to an imager's ability to detect varying amounts of it. If you design and build for ultimate sensitivity you necessarily produce a situation where a maximum detectable concentration is manifest. Anyone who is attempting to quantify concentrations under these conditions is bound to incur the physical barriers outlined above.

6. APPENDIX

The test methodology and experimental practices employed for the measurement of the camera's sensitivity threshold to methane were also utilized on other gases and in conjunction with different camera systems. In this appendix we give a brief overview of the gases and cameras tested and the results of those tests.

The first gas shown is Ethylene. It is flowed in the same manner as the methane described above. The same IR camera system used in the methane testing is utilized in this ethylene test. Figure 9

shows the transmission of Ethylene and Figures 10 and 11 show the experimental results. We then proceed to review Carbon Monoxide. The CO gas is tested in the typical fashion with a camera system that is spectrally tuned for its particular absorption bands. The camera system used for the CO testing is not the same system that was used for ethylene or methane. The results are shown in figures 12 through 14.

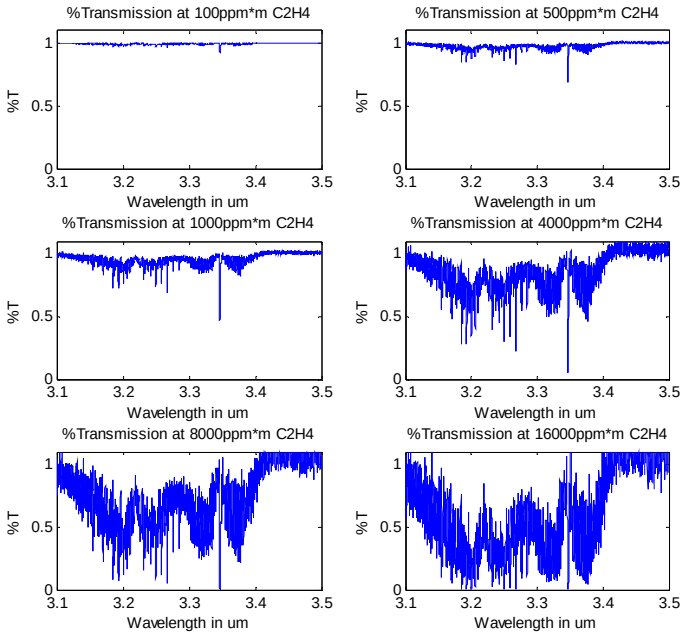

Figure 9. Spectral transmission approximations of Ethylene at various vapor concentrations.

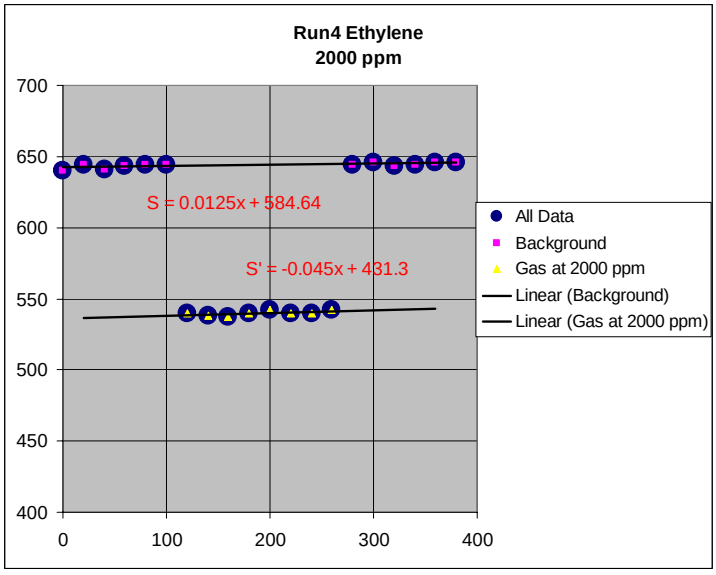

Figure 10. The signal change due to C2H4 at 2000ppm in the gas cell. Back grounds are taken before and after the gas release.

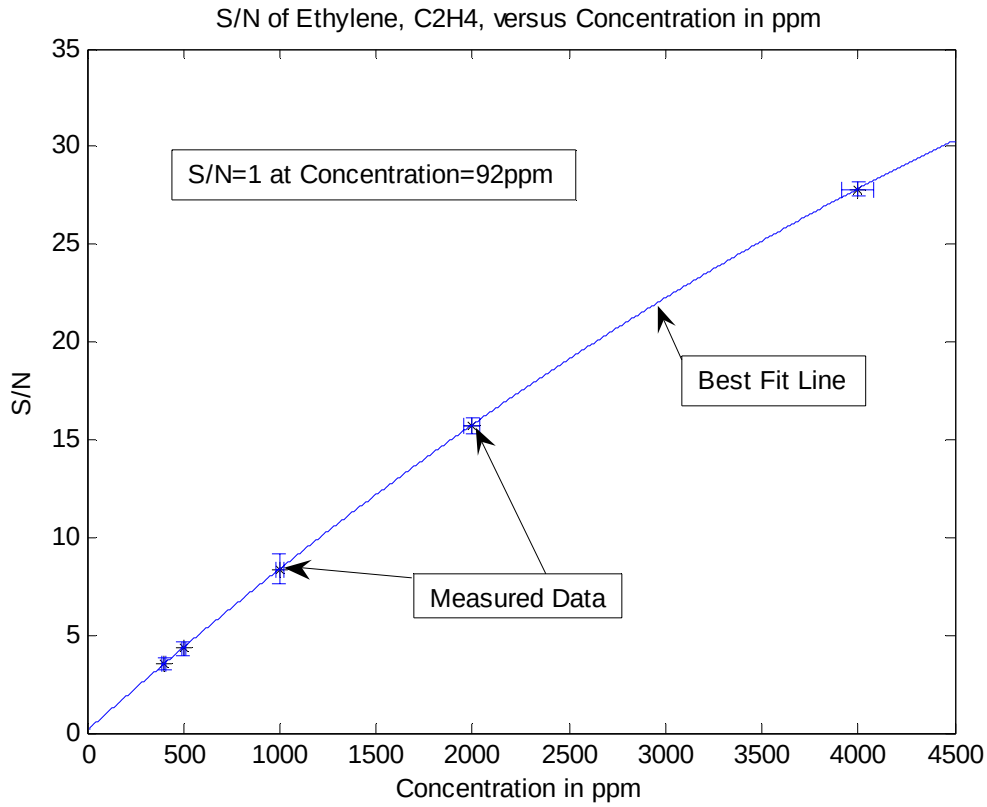

Figure 11. S/N versus Concentration of Ethylene. Best fit to a quadratic polynomial.

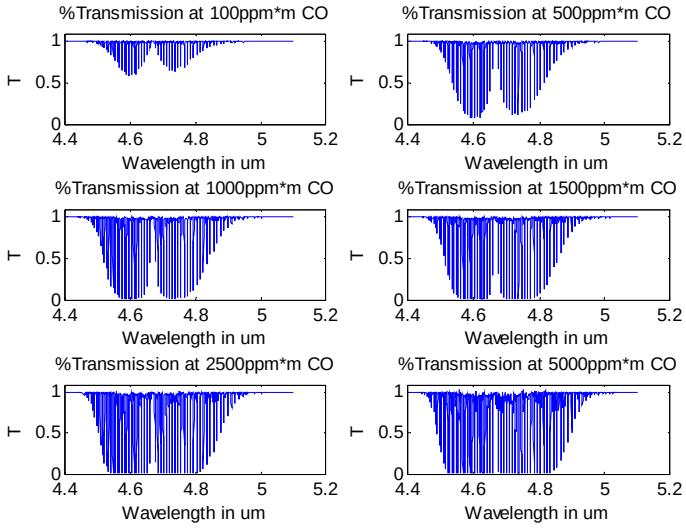

Figure 12. Spectral transmission approximations of Carbon Monoxide at various vapor concentrations.

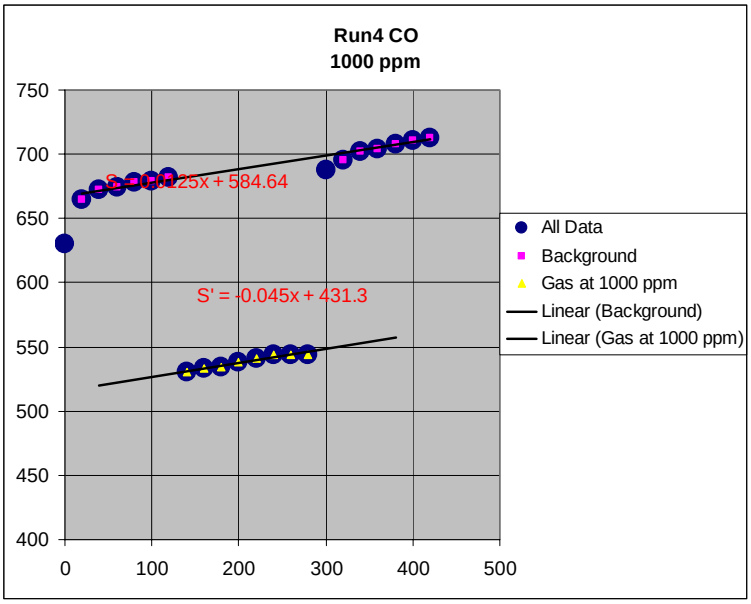

Figure 13. The signal change due to CO at 1000ppm in the gas cell.

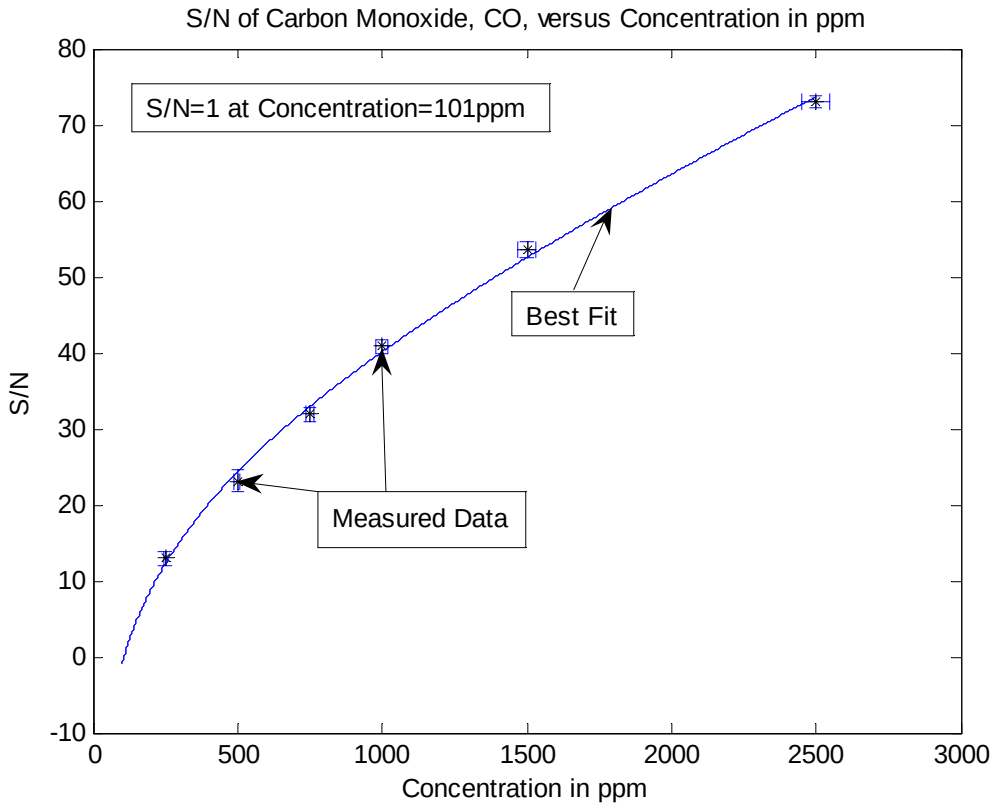

Figure 14. Signal to Noise versus Concentration of Carbon Monoxide. The data was fit to a transcendental function of the same form as the methane sample.

[1] **"STANDOFF PASSIVE OPTICAL LEAK DETECTION OF VOLATILE ORGANIC COMPOUNDS USING A COOLED INSB BASED INFRARED IMAGER", BENSON ET AL, AWMA PROCEEDINGS 2006.**

[2] **USEPA TECHNOLOGY TRANSFER NETWORK, ENVIRONMENTAL PROTECTION AGENCY, WWW.EPA.GOV/TTN**

[3] **"THE PHYSICS OF ASTROPHYSICS VOL#1 RADIATION",** PP. 3-7, FRANK H. SHU, UNIVERSITY SCIENCE BOOKS, 1991. MILL VALLEY, CA.

[4] **"POISSON PROCESS AND SHOT NOISE: PROBABILITY, RANDOM VARIABLES, AND STOCHASTIC PROCESSES", PP 554-576, PAPOULIS, A., MCGRAW-HILL, NY,NY. 1984.**

[5] **ENVIRONICS 4000 MULTICOMPONENT GAS MIXING SYSTEM, TOLLAND, CT. HTTP://WWW.ENVIRONICS.COM/4000.HTML**

[6] **MATLAB CURVE FITTING TOOLBOX, MATHWORKS, NATICK, MA. HTTP://WWW.MATHWORKS.COM/PRODUCTS/CURVEFITTING/**